LETTERS TO NATURE

Abscisic acid-induced elevation of guard cell cytosolic Ca^{2+} precedes stomatal closure

M. R. McAinsh*, C. Brownlee† & A. M. Hetherington*

* Institute of Environmental and Biological Sciences, Division of Biology, University of Lancaster, Lancaster LA1 4YQ, UK
† Marine Biological Association, The Laboratory, Citadel Hill, Plymouth PL1 2PB, UK

STOMATA allow the diffusion of CO_2 into the leaf for photosynthesis and the diffusion of H_2O out of the leaf during transpiration[1,2]. This gaseous exchange is regulated by pairs of guard cells that surround each stomatal pore. During water stress the loss of water through transpiration is reduced in response to abscisic acid[3], a naturally occurring plant growth regulator which is also present in certain mammals[4], algae[5] and fungi[6], by the promotion of stomatal closure and inhibition of opening[7]. This involves alterations to guard cell turgor, causing the cells to shrink and thereby reducing the size of the stomatal pore. These changes are driven by cation and anion effluxes[8]. It has been proposed that an abscisic acid-dependent increase in the concentration of guard cell cytosolic free calcium triggers the intracellular machinery responsible for stomatal closure[9] (for a review, see ref. 10), but attempts to test this hypothesis by measuring [^{45}Ca] fluxes have produced equivocal results[11]. Using the fluorescent calcium indicator fura-2, we report that abscisic acid induces a rapid increase in guard cell cytosolic free Ca^{2+} in *Commelina communis* L., and that this increase precedes stomatal closure. These results strongly support the suggestion that Ca^{2+} is an intracellular second messenger in this response.

Figure 1 shows a typical dose response to applied abscisic acid (ABA). The minimum concentration of (+/−) cis–trans ABA (10^{-6} M) that induces maximum stomatal closure was used in all subsequent experiments on the effect of ABA on guard cell cytosolic free calcium ([Ca^{2+}]$_{cyt}$). To monitor real time changes in [Ca^{2+}]$_{cyt}$ in single stomatal guard cells, we used the fluorescent calcium indicator fura-2[12]. Fluorescent indicators such as fura-2 and indo-1 have already been used successfully to monitor free calcium concentrations in root hairs[13] and aleurone layer protoplasts[14,15]. Preliminary experiments established that stomatal guard cells in common with other plant cells (but unlike many animal cells) would not take up the esterified form of this molecule. Additionally, the failure of the low-pH loading method, successfully used with plant protoplasts[15], necessitated that the dye be micro-injected into the cytoplasm using iontophoresis. Figure 2a shows a bright-field image of a stomatal complex, the right-hand guard cell of which has been loaded with fura-2. In Fig. 2b the same complex is

shown under fluorescence and it is apparent that the fura-2 has been loaded into the cytoplasm of the right-hand cell. Guard cells with fura-2 loaded into the cytoplasm remained viable throughout the course of the experiments and continued to respond to ABA by reducing their turgor. Furthermore, such cells retained dye in the cytoplasm with no obvious accumulation in the vacuole. By contrast, guard cells in which fura-2 had been loaded into the vacuole immediately lost turgor and the distribution of the dye appeared to be much more diffuse when viewed under fluorescence. These factors meant that we were able to reject any cells in which the dye was not loaded into the cytoplasm.

When guard cells previously loaded with fura-2 were perfused with 10^{-6} M ABA, there was an immediate increase in [Ca^{2+}]$_{cyt}$ (Fig. 3b); this increase preceded any detectable alteration in the aperture of the stomatal pore by at least 6 min (Fig. 3c). It was important that the [Ca^{2+}]$_{cyt}$ in untreated guard cells remained constant (Fig. 3a) and there was no alteration in the aperture of the stomatal pore. Using an in vitro calibration curve (see legend to Fig. 3), we estimate that resting [Ca^{2+}]$_{cyt}$ lies between 70–250 nM, with a mean of 115 ± 26 nM ($n = 10$). Eight out of ten guard cells responded to 10^{-6} M ABA with an increase in [Ca^{2+}]$_{cyt}$ (there was no increase or decrease in [Ca^{2+}]$_{cyt}$ in the remaining two cells). These responses represent an increase over resting [Ca^{2+}]$_{cyt}$ of between 2- and 10-fold. For example, in the response shown in Fig. 3, the [Ca^{2+}]$_{cyt}$ rose from a resting [Ca^{2+}]$_{cyt}$ of 70 nM to 600 nM, with peaks up to 1 μM, about 10 min after the addition of ABA. Variations in [Ca^{2+}]$_{cyt}$ which resemble oscillations were also apparent after ABA treatment (Fig. 3b). Interestingly, these are more similar in form to those in mammalian cells[16] than those induced by auxin in maize epidermal cells[17], but further investigation is necessary to characterize this phenomenon in stomatal guard cells.

The absolute values of 360 nm fluorescence (fura-2 excitation isosbestic point) for fura-2-loaded guard cells (Fig. 3d) showed no marked change following the addition of ABA. There was a slight decrease in fluorescence with time, which we attribute to either a gradual leakage of dye from the cell and/or dye bleaching, both of which are compensated for by the dual wavelength ratio measurements[12]. This confirms that the observed increases in [Ca^{2+}]$_{cyt}$ are not an artefact due to modification to the optical properties of the cell brought about by ABA or guard cell movement during stomatal closure.

MacRobbie observed a transient stimulation of ion effluxes in response to ABA (refs 11, 18) and has suggested that this could provide a mechanism by which increases in [Ca^{2+}]$_{cyt}$ might initiate stomatal closure. The similarity between the time course of these efflux transients[11,18] and the ABA-induced increase in [Ca^{2+}]$_{cyt}$ that we report here, strongly suggests that these two events are interrelated. Recent patch clamping studies[19,20] also help to explain the mechanism by which an increase in [Ca^{2+}]$_{cyt}$ might lead to a reduction in aperture of
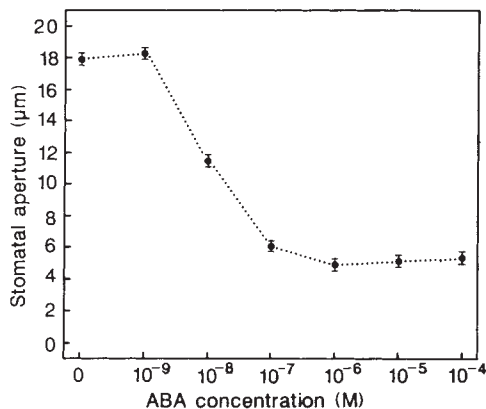

FIG. 1 Response of abaxial stomata of *C. communis* L. to a range of concentrations of abscisic acid (10^{-9}–10^{-4} M). Means of 90 measurements ± s.e. Maximum response was observed between 10^{-7} and 10^{-6} M ABA.
METHODS. Seedlings of *C. communis* L. were grown from seed[9]. Epidermis was peeled carefully from the abaxial surface of the youngest fully expanded leaf[22], floated on 10^{-2} M MES (2-[*N*-morpholino]ethane sulphonic acid; Fluka), pH 6.15, and cut into 5 mm lengths. To promote stomatal opening, pieces of epidermis were incubated for 3 h at 25 ± 1°C under a photon flux density of 200 μmol m^{-2} s^{-1} in 10^{-2} M MES, 5×10^{-2} M KCl, pH 6.15, aerated with CO_2-free air[9], after which (+/−) cis–trans ABA (Sigma) was added to the medium. Following incubation for 1 h in ABA, the epidermal strips were examined under the microscope to determine the aperture of the stomatal pores.
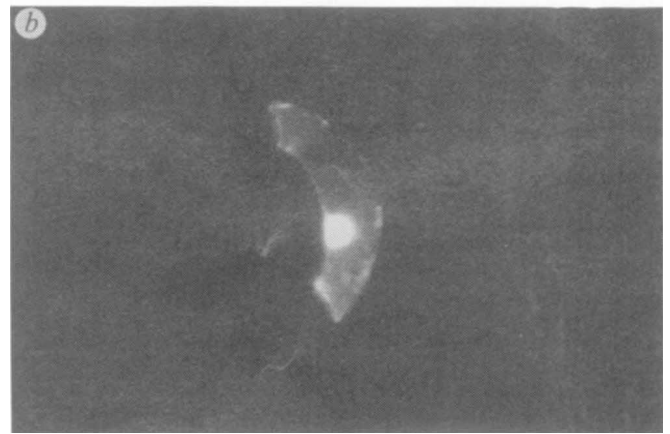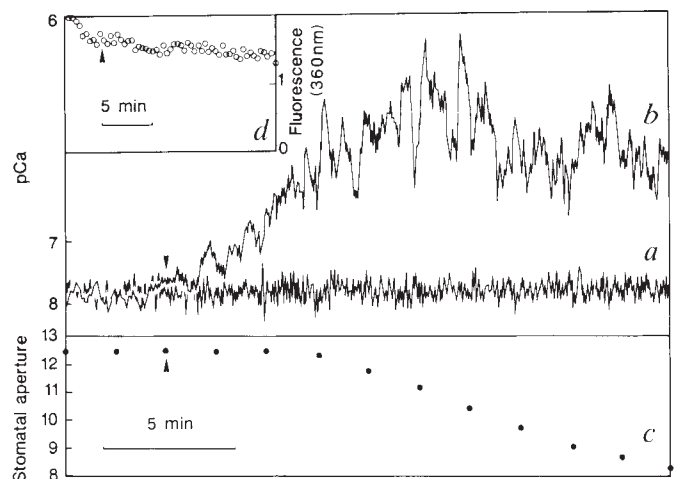
FIG. 2 *a*, Bright-field image of a stomatal complex from *C. communis* L. The diameter of the pore is 12 μm (see legend to Fig. 1 for methods). After loading with fura-2, the right-hand guard cell retained a constant aperture for 45 min and dye remained in the cytoplasm. *b*, Fluorescence image of the same fura-2-loaded guard cell as in *a*. Excitation was at 360 nm. Emission was monitored at 510 nm (see legend to Fig. 3).

METHODS. Epidermal strips of >2 cm in length were incubated under conditions promoting stomatal opening for 2–3 h (see legend to Fig. 1). Strips on which the stomata were open (12–15 μm) were mounted, cuticle down, on a glass coverslip and secured by smaller coverslips. The preparation was seated in a purpose-built perfusion cell on the microscope stage and the strip perfused continuously with CO_2-free 10^{-2} M MES, 5×10^{-2} M KCl, pH 6.15, at 25 °C. This treatment resulted in no alteration to the stomatal aperture. Fura-2 was microinjected iontophoretically. Guard cells were impaled with filamented glass microelectrodes (<0.25 μm tip diameter) containing 10^{-3} M fura-2 pentapotassium salt (Calbiochem) in their tips[23]. The electrodes were connected with silver/silver chloride wire to a microelectrode amplifier and stimulator. Current pulses (1.0 nA negative pulses, 2 Hz, 200 ms duration) were given for <30 s to load cells, giving a final estimated concentration of fura-2 in the cytoplasm of ~10^{-4} M (ref. 24). Following microinjection, the electrode was removed for fluorescence measurements. Fluorescence was observed with a ×40 water-immersion objective (Zeiss).

FIG. 3 Changes in guard cell $[Ca^{2+}]_{cyt}$ with time. *a*, Cells perfused with CO_2-free 10^{-2} M MES, 5×10^{-2} M KCl, pH 6.15, at 25 °C. *b*, Before and after addition of 10^{-6} M ABA (arrow). *c*, Changes in stomatal aperture with time, before and after addition of 10^{-6} M ABA (arrow). *d*, Changes in 360 nm fluorescence (fura-2 excitation isosbestic point) with time, before and after the addition of 10^{-6} M ABA (arrow).

METHODS. Stomatal guard cells of *C. Communis* L. were loaded with fura-2 (see legend to Fig. 2). Ca^{2+}-dependent fura-2 fluorescence was monitored with dual wavelength fluorescence microscopy[23,25–27]. Fura-2-loaded cells were observed with a modified M2 micromanipulation microscope (Microinstruments, UK), using a ×40 water-immersion objective (Zeiss). Excitation, using 360 and 385 nm light alternately, was provided from a 150 watt xenon lamp source by a fluid light guide (Microinstruments) in combination with a rotating filter holder. Fluorescence emission at 510 nm was monitored with a photomultiplier tube (PM9924B; EMI), the output of which was synchronized with the excitation source by a BBC microcomputer. Each fluorescence measurement was an average of 50 individual readings. Guard cell autofluorescence was measured at each wavelength before loading with fura-2. Autofluorescence subtraction and 360/385 nm ratio calculations were performed on-line during the experiment to give one ratio reading every 2 s. The aperture of the stomatal pore was determined *in situ* every 50 ratios (~100 s) using a calibrated eye piece micrometer. Values of pCa are based on *in vitro* calibration using drops of Ca^{2+}-calibration buffers containing 2×10^{-5} M fura-2 (ref. 28). We found that *in vivo* calibration with ionomycin[23,25,26] was not possible. No changes in $[Ca^{2+}]_{cyt}$ were observed in guard cells from epidermal strips incubated in solutions of ionomycin contain-

ing zero (10^{-3} M EGTA) or 10^{-2} M $CaCl_2$, pH 8.0. Furthermore, the combination of high $[Ca^{2+}]$ and ionomycin failed to induce stomatal closure and did not influence cytoplasmic streaming, which is known to be strongly Ca^{2+}-dependent[29].

the stomatal pore. An increase in $[Ca^{2+}]_{cyt}$ would be expected to block inward rectifying K^+ channels and hence inhibit stomatal opening, whereas closure might result from the activation of a calcium-stimulated chloride channel. The resulting chloride efflux could then depolarize the guard cell plasma membrane sufficiently to activate the outwardly directed K^+ channel[19,20].

In summary, we have reported that ABA induces an increase

in guard cell $[Ca^{2+}]_{cyt}$ which precedes stomatal closure. Our results provide an important link in the guard cell signal transduction chain. It will be of interest to determine whether opening stimuli, such as light and auxin, induce alterations to guard cell $[Ca^{2+}]_{cyt}$. Experiments using calcium-sensitive microelectrodes have revealed that light causes a decrease in $[Ca^{2+}]_{cyt}$ in *Nitellopsis*[19], and auxin causes an increase in $[Ca^{2+}]_{cyt}$ in maize[17]. Future

work will attempt to establish the site(s) of calcium entry into the cytosol, including the involvement of intracellular stores, and also to identify other components in the guard cell signal transduction chain. □

1. Raschke, K. in *Encyclopedia of Plant Physiology* New Ser. Vol. 7 (eds Haupt, W. & Feinleib, M. E.) 381–441 (Springer, Berlin, 1979).
2. Zeiger, E. A. *Rev. Plant. Physiol.* **34**, 441–475 (1983).
3. Davies, W. S. & Mansfield, T. A. in *Abscisic Acid* (ed. Addicott, F. T.) 237–268 (Praeger, New York, 1983).
4. Le Page-Degivry, M.-Th., Bidard, J.-N., Rouvier, E., Boulard, C. & Lazdunski, M. *Proc. natn. Acad. Sci. U.S.A.* **83**, 1155–1158 (1986).
5. Tietz, A., Ruttkowski, U., Kohler, R. & Kasprik, W. *Biochem. Physiol. Pflanz.* **184**, 259–266 (1989).
6. Assante, G., Merlini, L. & Nasini, G. *Experimentia* **33**, 1556 (1977).
7. Mittelheuser, C. G. & van Steveninck, R. F. M. *Nature* **221**, 281–282 (1969).
8. MacRobbie, E. A. C. in *Stomatal Function* (eds Zeiger, E., Farquhar, G. D. & Cowan, I. R.) 125–162 (Stanford University Press, California, 1987).
9. De Silva, D. L. R., Hetherington, A. M. & Mansfield, T. A. *New Phytol.* **100**, 473–482 (1985).
10. Mansfield, T. A., Hetherington, A. M. & Atkinson, C. J. *A. Rev. Pl. Physiol.* (in the press).
11. MacRobbie, E. A. C. *Planta* **178**, 231–241 (1989).
12. Tsien, R. Y. *A. Rev. Neurosci.* **12**, 227–254 (1989).
13. Clarkson, D. T., Brownlee, C. & Ayling, S. M. *J. Cell. Sci.* **91**, 71–80 (1988).
14. Bush, D. S. & Jones, R. L. *Cell Calcium* **8**, 455–472 (1987).
15. Bush, D. S. & Jones, R. L. *Eur. J. Cell Biol.* **46**, 446–469 (1988).
16. Berridge, M. S., Cobbold, P. H. & Cuthbertson, K. S. R. *Phil. Trans. R. Soc.* B **320**, 325–343 (1988).
17. Felle, H. *Planta* **174**, 495–499 (1988).
18. MacRobbie, E. A. C. *Bot. Acta* **101**, 140–148 (1988).
19. Schroeder, J. I. & Hedrich, R. *Trends Biochem. Sci.* **14**, 187–192 (1989).
20. Schroeder, J. I. & Hagiwara, S. *Nature* **338**, 427–430 (1989).
21. Miller, A. J. & Sanders, D. *Nature* **326**, 397–400 (1987).
22. Weyers, J. D. B. & Travis, A. J. *J. exp. Bot.* **32**, 837–850 (1981).
23. Brownlee, C. & Pulsford, A. L. *J. Cell Sci.* **91**, 249–256 (1988).
24. Purves, R. D. *Microelectrode Methods for Intracellular Recording and Ionophoresis* (Academic, New York, 1981).
25. Williams, D. A., Fogarty, K. E., Tsien, R. Y. & Fay, F. S. *Nature* **318**, 558–561 (1985).
26. Poenie, M., Alderton, S., Steinhardt, R. & Tsien, R. *Science* **233**, 886–889 (1986).
27. Brownlee, C. *Biol. Bull.* **176**(s), 14–17 (1989).
28. Tsien, R. Y. & Rink, T. J. *Biochim. biophys. Acta* **599**, 623–638 (1980).
29. Williamson, R. E. & Ashley, C. C. *Nature* **296**, 647–651 (1982).

Role for the nitrogenase MoFe protein α-subunit in FeMo–cofactor binding and catalysis

Deborah J. Scott*, Harold D. May*, William E. Newton*†, Kevin E. Brigle‡ & Dennis R. Dean†‡

* Western Regional Research Center, USDA-ARS, Albany, California 94710, USA and Department of Agronomy and Range Science, University of California at Davis, Davis, California 95616, USA
‡ Department of Anaerobic Microbiology, Virginia Polytechnic Institute and State University, Blacksburg, Virginia 24061, USA

TWO components constitute Mo-dependent nitrogenase (EC 1.18.6.1)—the Fe protein (a homodimer encoded by *nifH*) and the MoFe protein (an $\alpha_2\beta_2$ tetramer encoded by *nifDK*). The MoFe protein provides the substrate-binding site[1–3] and probably contains six prosthetic groups of two types—four Fe-S centres and two Fe- and Mo-containing cofactors[4,5]. To determine the distribution and catalytic function of these metalloclusters, we[6,7] and others[8] are attempting to change the catalytic and spectroscopic features of nitrogenase by substituting specific amino acids targeted as potential metallocluster ligands, particularly those to the FeMo-cofactor, which is responsible for the biologically unique

electron paramagnetic resonance signal ($S = \frac{3}{2}$) of nitrogenase[9,10], and is believed to be the N_2-reducing site[11]. Here we describe mutant strains of *Azotobacter vinelandii* that have single amino-acid substitutions within the MoFe protein α-subunit. These substitutions alter both substrate-reduction properties and the unique electron paramagnetic resonance signal, indicating that the FeMo–cofactor is associated with both the α-subunit and the substrate-reducing site.

Nitrogenase MoFe proteins all have a very high level of primary sequence identity. To target appropriate residues for substitution, we correlated the chemical nature of the denaturing solvents that are effective in extruding each type of metallo-cluster with comparisons of interspecies and intersubunit amino-acid sequences. Residues targeted for substitution include certain strictly conserved cysteine and histidine residues[7] that could respectively serve as thiol or N-donor ligands to the FeMo–cofactor. Histidine residues are known to ligand protein-bound Fe-S clusters[12]. Also, metallocluster extrusion requirements[9,13], electron spin echo[14] and Fourier transform infrared analyses[15] indicate one or more deprotonated nitrogen ligands to the FeMo–cofactor.

Primary sequences of those *nif*-specific gene products required for the biosynthesis of the FeMo-cofactor have also been examined to gain an insight into the possible nature of the binding domains for the FeMo-cofactor that are located within the MoFe protein. For example, we have suggested that the products of two such FeMo–cofactor biosynthetic genes, *nifE* and *nifN*, form a scaffold on which the FeMo-cofactor is assembled[16]. Indeed, the *nifE* and *nifN* gene products have considerable identity with the MoFe protein α- and β-subunits, respectively[16–21]. Also, the *nifEN* gene products form a tetrameric complex[22] analogous to the MoFe protein. Because the FeMo-cofactor must escape from the NifEN biosynthetic complex during maturation of the MoFe protein, the respective FeMo-cofactor-binding sites of the MoFe protein and NifEN are likely to be structurally similar but functionally inequivalent. We, therefore, substituted histidine 195 of the MoFe protein α-subunit with the corresponding residue of the *nifE* gene product, asparagine (Fig. 1). In this way, we expected to alter the functional character of a potential FeMo-cofactor environment without severely altering the global polypeptide structure. We incorporated amino-acid substitutions using site-directed mutagenesis and a gene replacement procedure[6].

The resulting *A. vinelandii* mutant strain (DJ178) had a Nif⁻ phenotype. We compared the catalytic activity of its altered nitrogenase with that of native nitrogenase from the isogenic wild-type strain. In an atmosphere of 10% acetylene, wild-type crude extracts catalysed the reduction of acetylene to ethylene with no trace of ethane production. By contrast, the nitrogenase in crude extracts of DJ178, under identical conditions, produced ethane as well as ethylene, with ethane accounting for 35% of the electrons going to these products (Table 1). In addition,

```
                         *  *  *      *  *  *  *  *    ↓        ↓
                                                    *  *  *  *  *
MoFe protein α-subunit  180– P V R C E G F R G V S Q S L G H H I A N D A –201
nifE gene product       150– P V D S A G F Y G – T K N L G N R I A G E A –170
                              *  *     *        *        *
```

FIG. 1 Comparison of the amino-acid sequences of the *A. vinelandii* MoFe protein α-subunit[30] and the deduced *nifE* gene product sequence[17] in the region relative to the His 195 → Asn and Gln 191 → Lys substitutions in the α-subunit. Numbers refer to the residue position within the respective polypeptides. The initiating methionine is residue 1. Asterisks above the MoFe protein α-subunit sequence indicate residues that are conserved among all known MoFe protein α-subunit sequences. Asterisks below the *nifE* gene product sequence indicate residues that are conserved among all known *nifE* gene product sequences. Amino acids conserved between the *A. vinelandii* MoFe protein α-subunit sequence and the *nifE* gene product sequence are boxed. ↓, Gln and His residues substituted by the corresponding *nifE* gene product residue in the study described here.